CONF-781033--15

LA-UR-78-2711

TITLE: EVALUATION OF LMFBR FUEL-MOTION DIAGNOSTICS INSTRUMENTATION WITH PARKA

AUTHOR(S): A. E. Evans, Jr., Q-14
J. D. Orndoff, Q-14
W. L. Talbert, Jr., Q-14

SUBMITTED TO: The 1978 IEEE Nuclear Science Symposium to be held October 17 thru 20, 1978.

los alamos
scientific laboratory
of the University of California
LOS ALAMOS, NEW MEXICO 87545

An Affirmative Action/Equal Opportunity Employer

Form No. 836
St. No. 2629
1/75

UNITED STATES
ENERGY RESEARCH AND
DEVELOPMENT ADMINISTRATION
CONTRACT W-7405-ENG. 36

EVALUATION OF LMFBR FUEL-MOTION DIAGNOSTICS INSTRUMENTATION WITH PARKA*

A. E. Evans, Jr., J. D. Orndoff, and W. L. Talbert, Jr.

University of California, Los Alamos Scientific Laboratory,
Los Alamos, New Mexico 87545

Summary

To aid in the design of LMFBR safety test experiments and safety test facilities (STF), a program of evaluation of concepts for fuel-motion diagnostics instrumentation has been undertaken. A part of this evaluation is being done at PARKA, a Rover project critical assembly which has been modified to study the self nuclear image from driven FTR-type fuel assemblies. Feasibility of obtaining fast-neutron images of single-pin voids in assemblies of up to 127 fuel pins has been demonstrated, albeit marginally for the larger fuel bundles. The feasibility of using in-core detectors as fuel-motion monitors has also been studied. Use of PARKA in a pulsed mode to study STF transient phenomena is discussed.

Introduction

For the evaluation of the safety of fast breeder reactors, it is necessary to develop facilities where bundles of LMFBR fuel pins may be driven to destructive, accident-simulating conditions and to observe the motion of the test fuel during and subsequent to the reactor transient. Concepts being studied as candidates for fuel and clad-motion monitoring in these experiments include flash-x-ray cinematography,[1] single-and multiple-pinhole self radiography,[2] radiography with Fresnel and other coded apertures,[3] use of networks of in-core radiation detectors,[4] and the use of multi-aperture collimating hodoscopes.[5] The selection of a fuel-motion monitoring system must be done in advance of design of the test facility because the monitoring system selected will strongly influence facility requirements.

Criteria have been established[6] for the performance of fuel and clad-motion measurement systems. These criteria are based upon requirements for sensitivity, accuracy, and time and spatial resolution necessary to derive useful information from tests intended to simulate various types of core-disruptive accidents in fast reactors, and include specifications for field of view, spatial resolution, time duration and resolution, and density resolution. In general, the requirements vary with the size of the assembly undergoing test. For instance, horizontal spatial resolution requirements vary from 2 mm for tests of a few pins to 50 mm for multiple subassemblies which may contain over 1000 pins. The fuel-motion measurement system will also be required to have a capability for depth measurement comparable to its horizontal resolution, and be able to detect the movement of as little as 0.04 g of fuel in small-bundle tests or 50 g in multiple-subassembly tests. Time-resolution requirements vary from 0.2 msec to 100 msec depending upon the particular type of test to be performed.

Since the test assemblies are immersed in liquid sodium, the system is constrained to use the image formed by neutrons or gamma rays emitted by the assembly or x-rays transmitted through the assembly. The quality of this image is strongly influenced by scattering and by absorption within the test assembly of radiation emitted not only by the test assembly but also by the reactor which is used to drive the test assembly to destruction. The time resolution, or the minimum time during which information must be gathered to obtain an image with required spatial and density resolution, is limited ultimately by the statistics of radiation emission from the test assembly. However, for most practical cases, time resolution is limited either by the data-acquisition system in the case of radiation-counting systems or by mechanical or electronic considerations in the case of photo-imaging systems. The evaluation described herein is concerned only with the spatial and density resolution of static images obtainable for various test assemblies.

The Facility

The modified PARKA critical assembly has been described previously.[7] To recapitulate, PARKA is a Rover Project Kiwi reactor fueled with graphite-enriched UO_2 elements. The active core, of size 89-cm diameter by 132-cm height, is surrounded by a Be reflector containing 12 boron-loaded rotary control drums. Modification for the STF program included removal of 37 of the 1.9-cm (across flats) hexagonal fuel elements and replacement by a steel-lined chamber capable of holding from 1 to 127 fully enriched UO_2 fuel pins of FFTF dimensions. The removable 5.8-mm diameter test fuel pins are held 7.49 mm between centers in a hexagonal array by

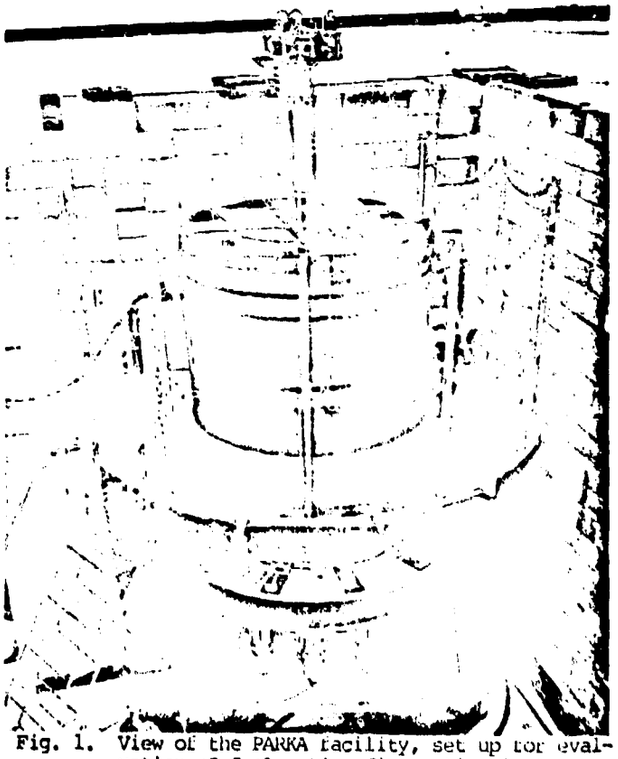

Fig. 1. View of the PARKA facility, set up for evaluation of fuel motion diagnostics instrumentation. The assembly at the top of the core is an actuator for remote rotation of test assemblies and withdrawal of individual fuel pins. The rotary reactor control-drive actuators can be seen on the underside of the reactor.

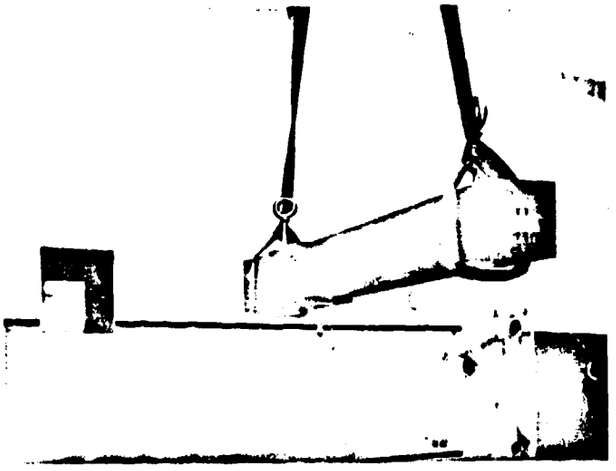

Fig. 2. Installation of four-channel hodoscope collimator.

aluminum grid plates in such a way that either individual pins or the entire test bundle can be removed from the reactor. Precision vertical and rotary actuators have been provided to permit remotely controlled movement of items in the test chamber. PARKA is shown in Fig. 1 after installation of the test actuators and extra lead shielding. A 4.4-cm wide by 10-cm high slot has been cut transversely through the fuel and the Be to permit viewing the test area with either a hodoscope or a coded-aperture viewing system. A second slot 4.5-cm wide by 5-cm high, located in the reflector 30 cm below the primary slot, is available for future experiments.

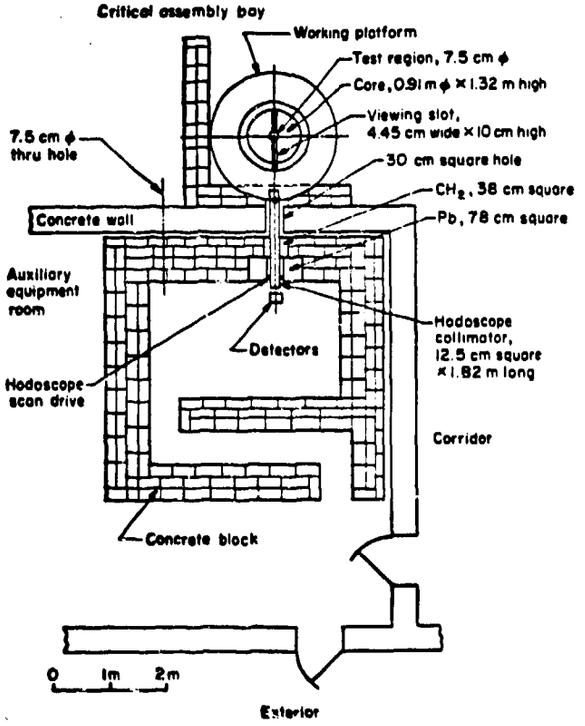

Fig. 3. Layout of the fuel-motion diagnostics instrumentation evaluation facility.

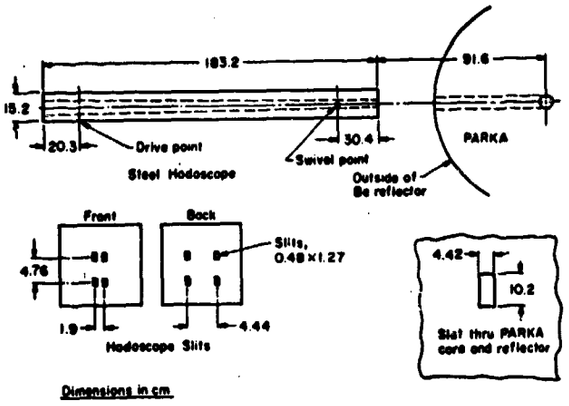

Fig. 4. Details of geometry of the hodoscope system.

A 4-channel steel hodoscope collimator is used to view the central region of the test chamber. The collimator, shown in Fig. 2, is installed in a hole through 2 meters of concrete separating the reactor area from a shielded instrumentation room in which the hodoscope detectors are located. The facility layout is shown in Fig. 3.

Details of the collimator and its relationship to the test region are given in Fig. 4. The slots through the collimator are 4.7-mm wide x 12.5-mm high. The front face of the collimator is 0.91 m away from the center of the reactor test region, with the result that the viewing area of each slot is 7-mm wide by 19-mm high (we define viewing area as the region bounded by the lines at which radiation from the test area seen by the hodoscope detectors falls to half of maximum intensity). The slots converge horizontally to view adjacent 7-mm-wide cells, but are parallel in the vertical direction.

The hodoscope is mounted to move horizontally about a point 25 cm from its front face, driven remotely by a precision machine slide and stepping motor on the back end. This permits scanning of the test section to simulate fuel motion, in lieu of the multichannel counting of a TREAT-type hodoscope. Scanning experiments are very much simplified by an automatic power-level control on PARKA which holds the reactor power level to within 0.1% over periods of several hours.

PARKA was selected for these studies because it is neutronically and geometrically similar to driver reactors which have been proposed for safety test facilities, and because it is a flexible system in which changes may be made easily. An epithermal to fast neutron spectrum is needed for such reactors in order that the test specimen is fairly uniformly irradiated. At the same time, it is necessary that the fission density in the test specimen be much higher than in the driver, so that in an actual test the test specimen may be driven to destruction without harming the driver reactor. The high ratio of fission density in the test region to fission density in the driver, referred to as figure of merit (FOM) also helps in improving the signal-to-background ratio in fuel-motion diagnostics measurements. The high FOM is obtained by fueling the test object with fully enriched uranium, either as pure metal or oxide, and maintaining a relatively low fuel density (400 kg/m^3 near the center of PARKA) in the driver.

Figure 5 shows the results of a ONETRAN[8] calculation of the fission density in the reactor

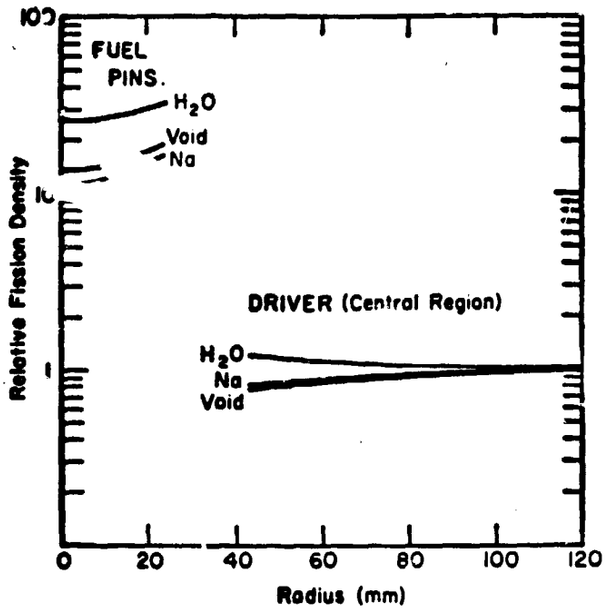

Fig. 5. Ratio of fission density in the test region of PARKA to that in the driver region for 37 test pins and various fillers.

for a 37-pin test array in PARKA, using water, sodium, and no filler between the pins. It is noted that use of water as a filler in this case improves the FOM by a factor of 2, a situation which can be taken advantage of when an experiment is performed where only gamma-ray information is desired. For fast-neutron self imaging of the fuel bundle, the presence of water would probably be intolerable. For single-pin experiments it has been shown possible to increase the FOM to as high as 80 by use of a polyethylene flux trap just outside of the test region. It is also noted that there is very little difference between sodium and void as fillers in the test region. Most of our tests have been done using aluminum grid blocks as a substitute for sodium.

Power distribution measurements have been made for 37-to 127-pin hexagonal fuel bundles in the test region of PARKA. The results are shown in Fig. 6. These measurements were made by irradiating fresh fuel pins in selected positions as the test assembly was built up from minimum to maximum size. The

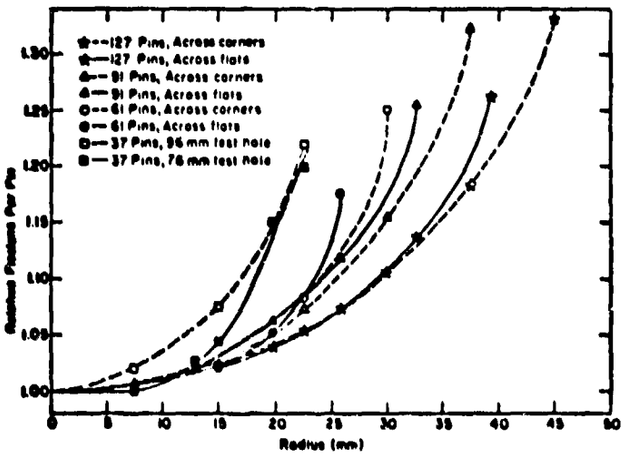

Fig. 6. Measured fission distributions of various-sized FTR fuel pin bundles in PARKA.

selected fuel pins were then removed, and the gross fission-product gamma activity of each pin was compared to the activity of the central pin which was used as a reference. The results show that, while the variation in power density across a test assembly is correctable in most cases, it will be a factor in interpreting fuel-motion diagnostic data. Graded fuel loading or graded fuel enrichment could be used where a more uniform power density is required in the test assembly.

Instrumentation

A number of detectors have been used with the collimator to measure the pattern of radiation emitted by the test section. For detection of fast neutrons, Hornyak Buttons[9] similar to those used on the TREAT hodoscope[5], ^4He recoil proportional counters[10] and stilbene scintillation detectors have been used. Experience has shown that the ideal neutron detector for this purpose is one which is as insensitive to gamma radiation as possible and can be biased for neutrons with energies of from 1 to 2 MeV. The detector should have a sensitive area closely matching the slot size in order to minimize backgrounds. The Hornyak buttons and ^4He recoil detectors have been found to meet the criteria of gamma insensitivity and energy discrimination. However, stilbene detectors are more efficient by a factor of 5 than Hornyak buttons of the same size and offer the additional advantage of pulse-shape discrimination,[11] by which it is possible to obtain simultaneously neutron and gamma-ray data.

A block diagram of electronics used with the stilbene detectors is shown in Fig. 7. The crystals, size 12.5-mm square by 6.2-mm thick, were imbedded edgewise in Lucite light pipes so as to couple geometrically with the hodoscope slots. The scintillator assemblies were viewed by Amperex type XP1110 photomultiplier tubes, the signals from which were passed through ORTEC type 113 preamplifiers, 300-m of type RG63/U cable from the critical assembly building to the control room and then through ORTEC type 460 delay-line-shaping amplifiers. The outputs of the amplifiers were analyzed for rise-time distribution using ORTEC model 458 pulse-shape analyzers.

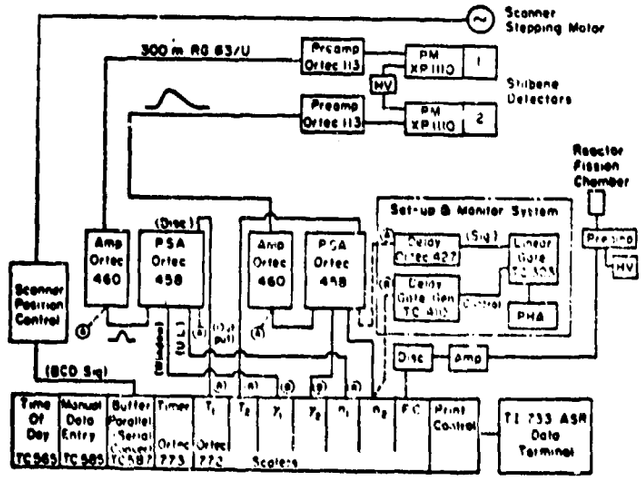

Fig. 7. Electronic system used for hodoscope scanning with stilbene detectors.

The pulse shape analyzer gives an output pulse with amplitude proportional to the 10-90% risetime of the incoming signal. Figure 8 is a comparison of

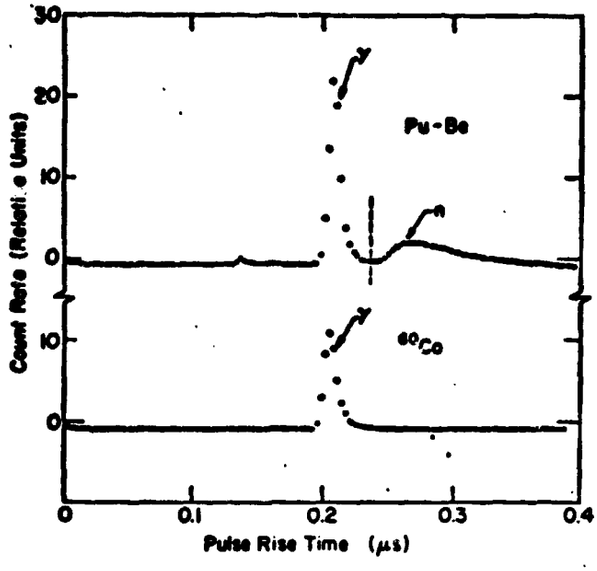

Fig. 8. Pulse-risetime distributions from stilbene detectors for a ^{238}Pu-Be neutron source and for a ^{60}Co gamma-ray source.

risetime distributions obtained with a ^{238}Pu-Be neutron source and with a ^{60}Co gamma-ray source. For this test, the input discriminator of the pulse-shape analyzer was set to accept pulses greater in amplitude than 1/2 the Compton edge from 662-keV ^{137}Cs gamma rays. The equivalent neutron energy threshold is 1.3 MeV. The independence of pulse-risetime distributions on neutron and gamma-ray energies and the resultant stability of the n-γ discrimination point (the minimum between the gamma-ray and neutron distributions) was checked by comparing the response to reactor radiation as seen through the hodoscope with that observed for Pu-Be neutrons.

Some earlier data were taken with Hornyak button scintillators, providing us a direct comparison with data obtained at TREAT. These detectors are the same size and mounted edgewise in lucite light pipes in the same way as the stilbene detectors. Pulse-height distributions for monoenergetic neutrons

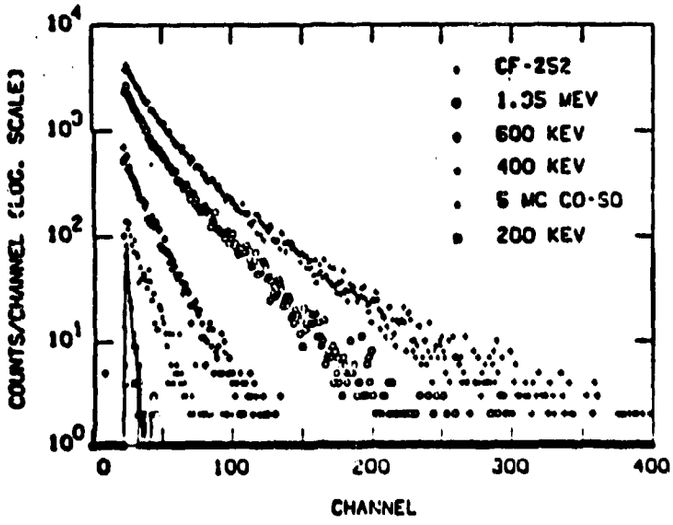

Fig. 9. Pulse-height distributions from a Hornyak button for neutrons of various energies and for an intense gamma-ray source.

incident upon these detectors are shown in Fig. 9. The detectors were tested at the LASL 3.75-MeV Van de Graaff Accelerator Facility using neutrons from the ^{7}Li(p,n)^{7}Be reaction. For use on the hodoscope, amplified signals from these detectors were counted using a discriminator setting just higher than that point at which counts were registered from a 5-mC ^{60}Co source held adjacent to the detector.

Hodoscope Scanning Results

Figure 10 shows the result of scanning across a single fuel pin with two detectors in the same horizontal plane. The detectors were Hornyak buttons. The reactor was operated at 550 W (4.6 mW/g ^{235}U). Each point took 500 sec of counting time. The signal-to-background (S/B) ratio for the single pin in this case is only 0.2:1 as compared to a typical S/B ratio of 3:1 for the TREAT hodoscope. The low S/B ratio of our hodoscope results from the epithermal neutron spectrum of PARKA. Since TREAT is a thermal reactor, its driver neutrons are on the average easier to separate from the fast neutrons emitted from the test region. The harder driver spectrum will be needed to produce uniform excitation across larger fuel-pin arrays; this demonstrates the need to verify the capability of the hodoscope technique before incorporating this technique into the design of safety test facilities for large-bundle tests.

The scan shown in Fig. 10 was made with the viewing slot extending only halfway through PARKA. The single-pin S/B ratio has since been improved by extending the slot through the reactor so that the collimator slots do not "see" any PARKA fuel. This is shown in Fig. 11. The S/B ratio has been improved by a factor of 3 as a result of the slot extension. This indicates the possible need for through slots for either hodoscope or coded-aperture imaging in safety test facilities. However, the through slot may not be of value for full subassembly or larger tests where the signal from the test bundle itself may dominate the driver background.

Also to be noted in Fig. 11 are the high counts on the right side of the curve. These are due to scattering from a piece of aluminum channel placed in the extended PARKA slot to support the fuel elements above the slot. This channel has since been replaced with a lighter, symmetrical support.

The next step was to see whether one missing pin in a 37-pin array could be detected. The results of this test are shown in Fig. 12. For this figure, each data point required 200 sec of counting time. The missing pin results in a 6% loss of count rate

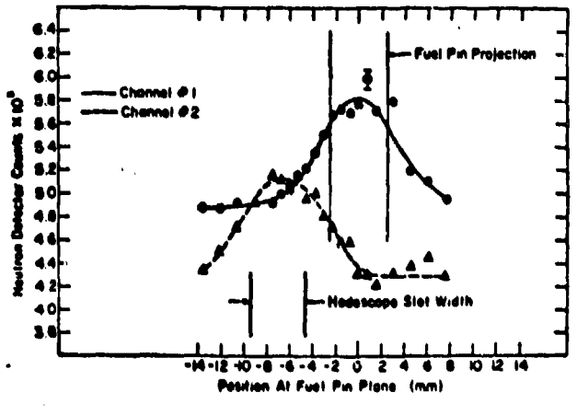

Fig. 10. Results of a 2-channel scan of a single fuel pin in PARKA, with the viewing slot extending only to the center of the core.

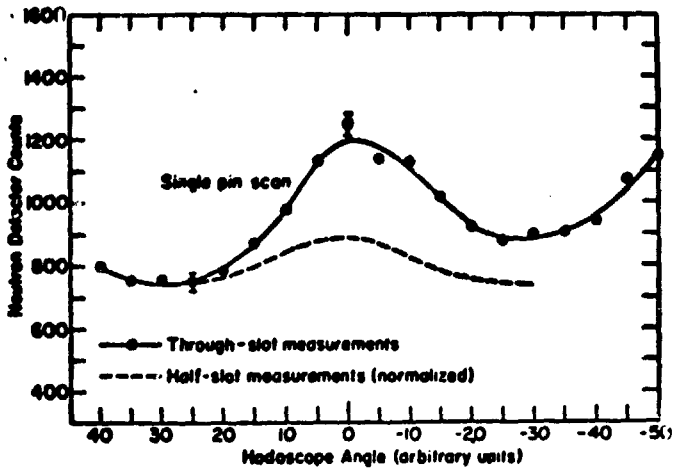

Fig. 11. Comparison of single-pin scans before and after extending the viewing slot all the way through the PARKA core.

over a distance consistent with the pin diameter and the geometrical resolution of the hodoscope. It should be noted that the absolute count rate difference between the 37-pin scan and the 36-pin scan at the center of the missing pin is about 40 percent of the net count from a single pin (Fig. 11). PARKA power levels were identical for the single and 37-pin experiments. This indicates the degree that neutron scattering and absorption may be expected to influence imaging results.

The 37-pin experiment was repeated after doubling the thickness of steel around the test array to 12.7 mm and filling the space between the fuel pins with drilled aluminum discs. The aluminum is a reasonable neutronic substitute for sodium. The result was little different from that obtained previously. There was an approximate 10% drop in total counting rate, but no apparent loss in resolution.

In a joint experiment with Argonne National Laboratory, a 91-pin EBR-II fuel bundle was scanned which had within it six missing fuel pellets, three of which were replaced by steel pins and three by air gaps. By rotating the bundle, scans could be made simultaneously through three of the defects, which were lined up on a major diameter of the hex pattern, or across the center defect alone either across flats or across corners of the hex. By using two vertical channels of the hodoscope, scans could be made through a perfect section of the assembly simultaneously with a faulted section. Both stilbene detectors and Hornyak buttons were used.

There will be more about the 91-pin test in a separate paper.[12] However, the results of one scan are shown here in Fig. 13. In the 3 curves are displayed the results of scanning neutrons of energy above 1 MeV, gamma rays of energy above 0.3 MeV, and the total (n+γ) outputs of the detectors. The data points are the counting ratios of one detector scanning across a normal section of the fuel bundle and the other detector scanning a section with a missing pellet in the middle of the assembly. The neutron scan shows a clear 3.5% difference in counter ratios over the diameter of the missing pellet (counter sensitivities were not normalized, so the base-line ratio is not 1). It is also clearly seen that the gamma-counting ratio does not reveal the missing pellet. As should be expected, summing the gamma-ray and neutron data serves only to dilute the neutron data, degrading the sensitivity of the hodoscope.

The absence of information in the 91-pin gamma scan was of concern because it reflects upon the ability to image defects in an assembly of this size by any technique which detects gamma rays produced in the assembly. We therefore went back and looked at the 37-pin assembly with stilbene, NaI(Tl) and NE102 detectors.

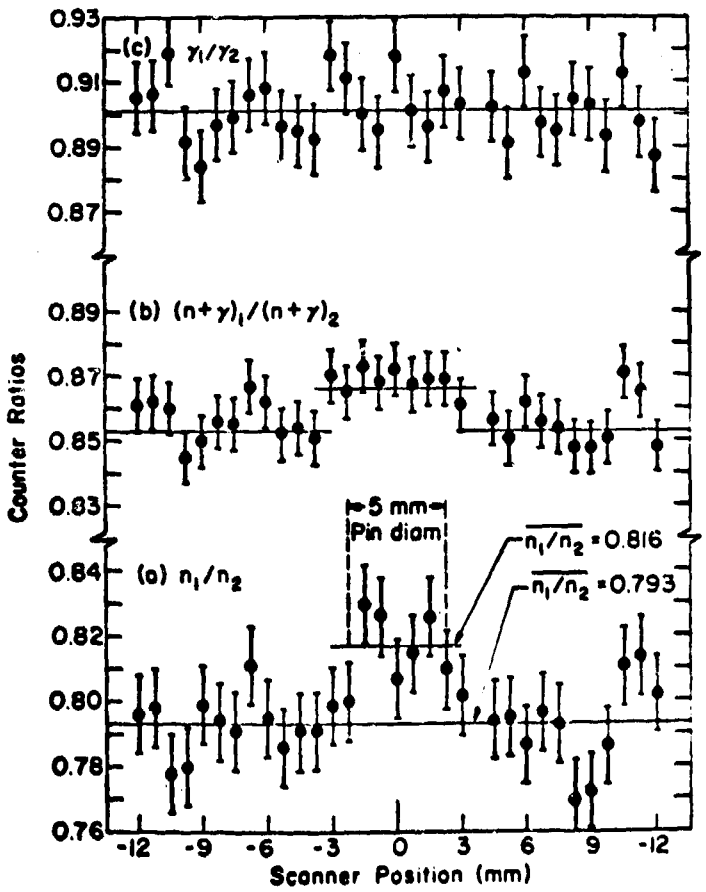

Fig. 13. Stilbene neutron, gamma, and total scan ratios across a faulted 91-pin EBR-II assembly. Counter ratios are of counts from a detector scanning across flats of a normal section of the assemby versus counts from a detector scanning across a section with a missiong pellet in the middle of the bundle.

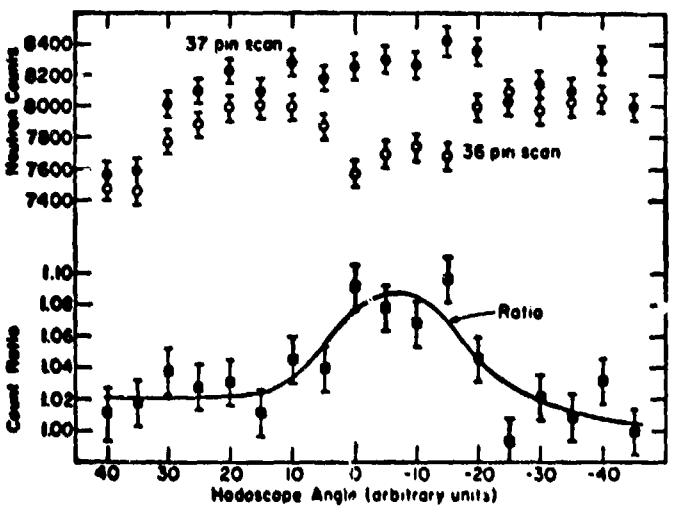

Fig. 12. Hodoscope scans with Hornyak buttons across flats of a 37-pin bundle, intact and with the central fuel pin withdrawn.

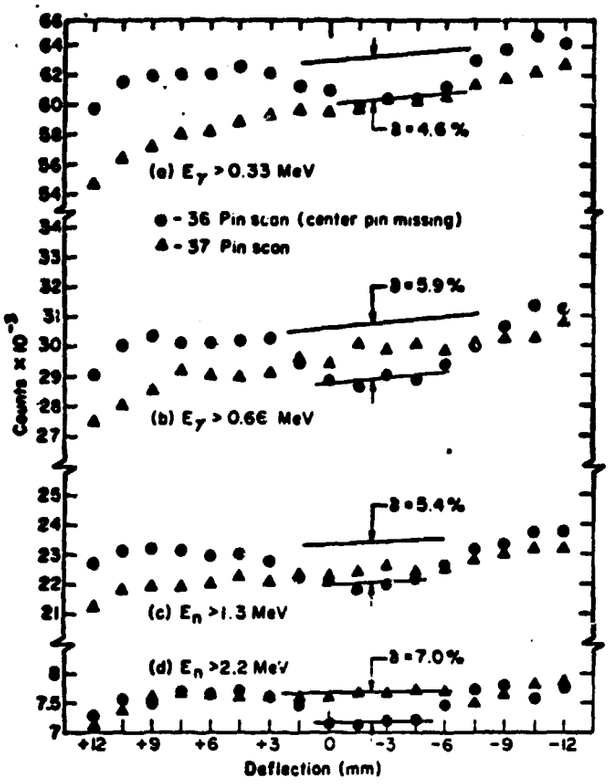

Fig. 14. Stilbene detector scans across flats of 37- and 36-pin assemblies.

The data for 37- and 36-pin scans with stilbene detectors are shown in Fig. 14. Using two detectors and two pulse-shape analysis systems, we obtained simultaneously gamma scans with (a) $E\gamma$ > 0.33 MeV and (b) $E\gamma$ > 0.66 MeV and neutron scans with (c) E_n > 1.3 MeV and (d) E_n > 2.2 MeV. (The neutron energies (c) and (d) correspond to the Compton edges for gamma-rays of energies (a) and (b) for equal pulse heights in stilbene.) In these scans, there is a left-to-right bias and an overall bias of the 37-pin scan with respect to the 36-pin scan because of the buildup of fission and activation products during the three hours in which these measurements were made. The 37-pin scan was done first, then the center pin was withdrawn and the scanner returned to the left-hand position to start the 36-pin scan. This is of course an effect of much less importance to the performance of multichannel hodoscopes, where all data are taken simultaneously, provided that power distribution and history are uniform across the test region. Time-of-count information could be used on these scans to correct for radiation buildup. The fact that the neutron scans show some buildup of counting rate during the run indicates some leakage of gamma counts into the neutron scalers. It appears that for a 37-pin assembly, gamma-ray information is somewhat inferior to fast-neutron information for fuel-motion de ection. The NaI(Tl) and NE102 scans were similar.

Using stilbene detectors biased as in the 37-pin tests, a 127-pin test assembly has been scanned with the hodoscope across flats and across corners of the hexagon, intact and with pins removed at various depths in the assembly. In Fig. 15 counting data are shown for scans across flats of the bundle intact and with the center pin withdrawn. Counts were for 200 s per data point at 5 mW/g^{235} U operating power (alternately expressed as counts/Joule/g^{235}U-a fortuitous choice!).

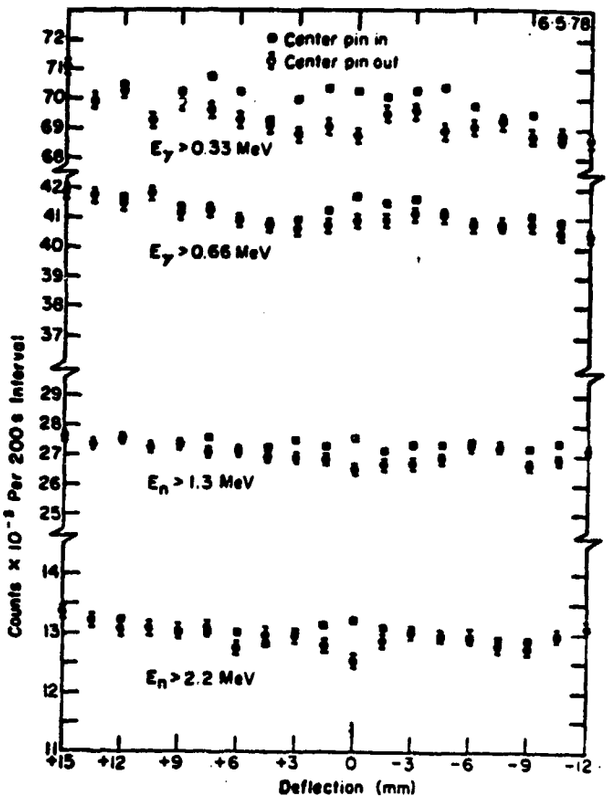

Fig. 15. Hodoscope scans across flats of a 127-pin bundle.

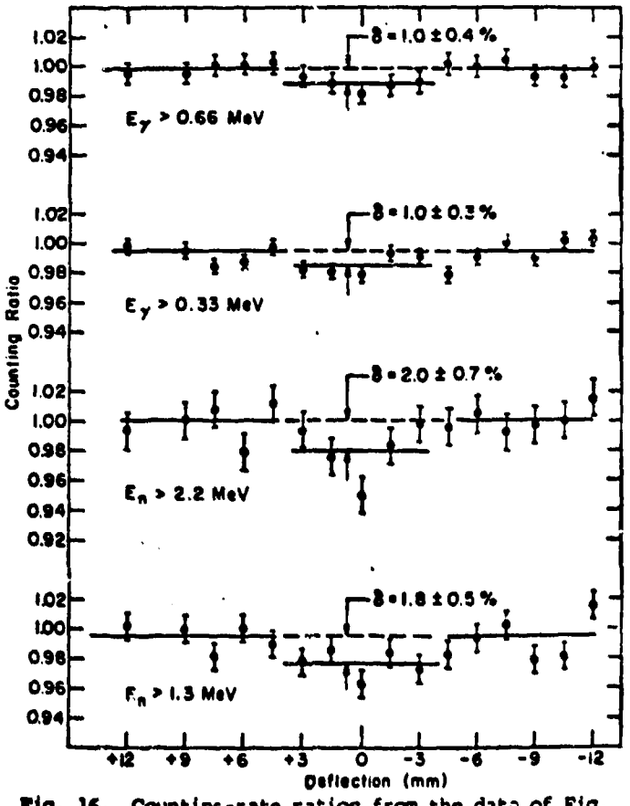

Fig. 16. Counting-rate ratios from the data of Fig. 15 to show the effect of a missing pin in the center of a 127-pin bundle.

To better observe the effect of withdrawing the pin, counting-rate pin-in to pin-out ratios are plotted in Fig. 16.

The fast neutron signal from the fuel in the center pin, averaged over the width of the pin, is ∿ 2% of the total count rate. The vertical resolution (to 1/2 intensity) of the hodoscope slot is 19.05 mm. This means that the observed count reduction was caused by the removal of 2.94 g of ^{235}U from the field of view, which is comparable to the established requirements for mass resolution for single subassembly tests.[6]

Fig. 17 shows the results of scanning with an apex of the assembly pointed towards the assembly. In this orientation, the rows of fuel pins are aligned in the direction of scanning, so that definite maxima and minima appear in the scan. Since the distance between rows of fuel is 6.29 mm and the field of view (to half-maximum intensity) of a hodoscope slot is 7.14 mm at the center of the test section, the hodoscope slot actually "sees" more fuel when the slot is pointed between two rows than when the slot is centered on a row of pins. As a result, a counting-rate minimum occurs when the hodoscope slot is pointed at a row of pins.

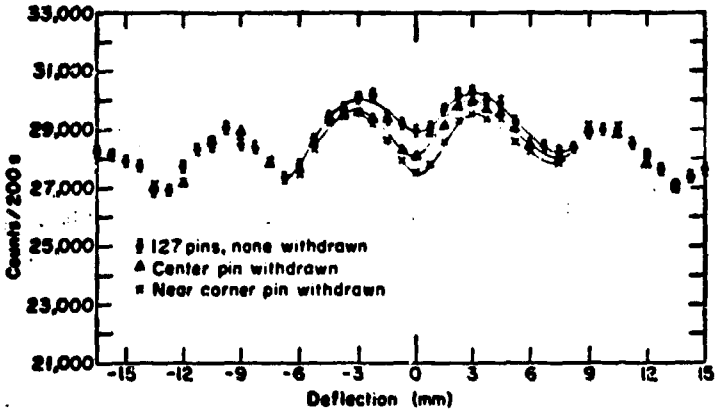

Fig. 17. Hodoscope scans across corners of a 127-pin fuel bundle. Detector was stilbene biased for neutrons > 1.3 MeV.

The figure shows the effect on the scan of withdrawing the central pin from the bundle and of withdrawing the corner pin nearest the hodoscope. Some of the difference in the response between the two pin locations is due to the power distribution within the assembly, discussed above. It is evident, however, that the response of the hodoscope to a void is not independent of the position of the void within the test assembly. In fig. 18 are plotted the results of scanning the assembly with a single missing pin at various depths within the bundle for both across-corners and across-flats scans. The data, taken with a stilbene detector biased for neutrons above 1.3 MeV, show that the total counting-rate reduction for a single-pin void in a 127-pin assembly varies from 3% for a void in the near edge of the assembly to 1% at the far edge. These data, which have been corrected for the measured power distribution within the assembly, show the need for a detailed static hodoscope study of every large bundle test before the destructive experiment is run. The need for 3-dimensional test data, as from crossed hodoscopes, is also evident.

Position dependence of void response has also been measured for a 37-pin bundle, for gamma radiation and neutrons. For fast neutrons, sensitivity losses from the front to the rear of the bundle ranged from 20 to 30%, depending upon neutron energy

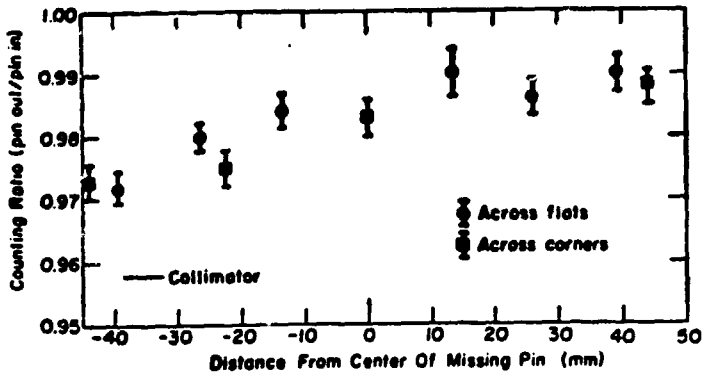

Fig. 18. Hodoscope sensitivity to a single-pin void as a function of the position of the void in a 127-pin test bundle. Stilbene detector, E_n > 1.3 MeV.

threshold. For gamma scans, the losses ranged from 35 to 50%.

In-Core Detector Tests

The PARKA system has been used for in-core detector studies. Initial studies were made with ^{235}U and ^{238}U fission chambers. These chambers, ∿ 5-mm in diameter, were fit into the stainless steel fuel-pin cladding tubes. Figure 19 is a cross sectional view of these detectors. The ^{238}U detector is sensitive to neutrons above 1 MeV and will thus respond primarily to neutrons from the test section. In contrast, the ^{235}U response weights the lower energy neutrons and is more sensitive to neutrons leaking into the fuel pin array from the driver.

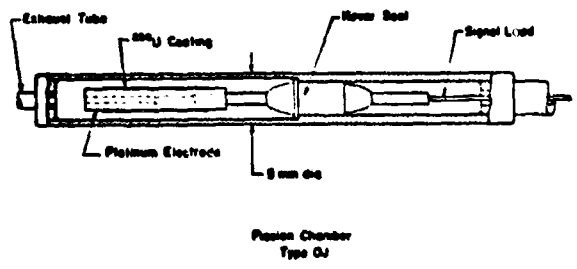

Fig. 19. Cross-sectional view of in-core fission detector. A detector of this type has also been used as an auxiliary power-level monitor for all hodoscope tests.

For a 37-pin test assembly, measurements have been made with the fission chambers located in the central fuel-pin cladding. Detector response was determined when fuel pins were removed from each of the three hexagonal rings of pins surrounding the detectors. Results summarized in Table 1 show that the ^{238}U detector counts decrease as the fuel pins are removed whereas counts from the ^{235}U detector increase. The $^{235}U/^{238}U$ counting ratio can be seen to be more sensitive to fuel loss than either detector separately. For these experiments, entire fuel pins were removed; however, it is expected that similar results would be obtained if short lengths were removed in the vicinity of the 10-mm active length fission detectors.

TABLE I

In-Core Fission Detector Response for Removal of Fuel Pins

Geometry	Relative detector counts		
	^{235}U	^{238}U	$^{235}U/^{238}U$
Six pins from ring 1	1.098	0.892	1.23
Six pins from ring 2	1.093	0.928	1.18
Six pins from ring 3	1.058	0.970	1.09

Results indicate that in-core detectors are capable of providing diagnostic information in multi-pin STF tests. It has been proposed that one or more fuel pins be replaced with "hardened" channels enclosing a line of alternate ^{235}U and ^{238}U fission chambers cooled by flowing argon gas. The ^{235}U detectors would then serve as monitors of the local neutron flux driving the fuel pins, while the ^{238}U detectors are sensitive to the proximity of fuel. For the high power levels in STF tests, ion current signals as a function of time would be preferable to counting rates.

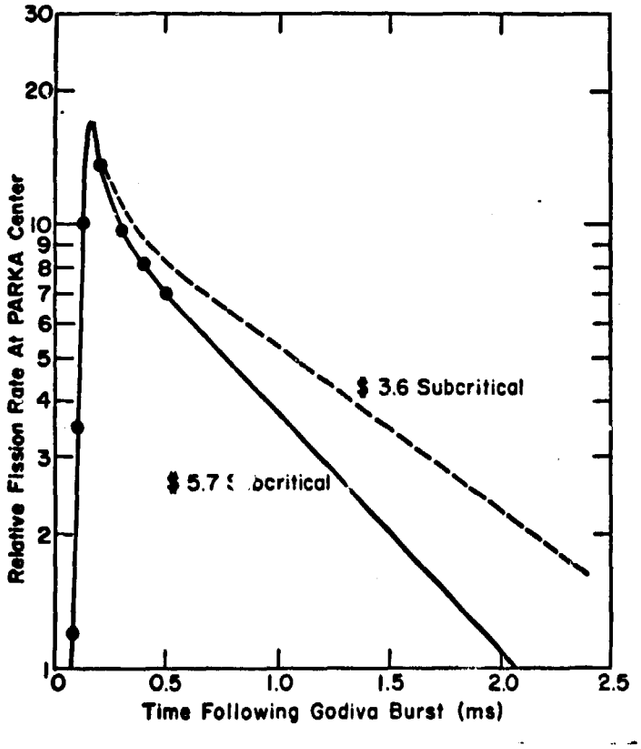

Fig. 20. PARKA response to Godiva bursts at two different PARKA reactivities.

Transient Operation

Hodoscope and in-core detector tests done using PARKA have been at low power and long counting times. While such an operating mode may be satisfactory for testing concepts involving nuclear counting instruments, it does not serve well for imaging experiments involving such concepts as coded apertures. Almost by accident, we have discovered a way in which PARKA might be used as a high-level, short-duration source. It was found that operation of Godiva, a prompt-burst reactor housed in the same experimental bay as PARKA, induced radiation levels in PARKA for a single burst event which were comparable to those which had been induced by a previous 10-minute, 55-watt power-calibration run. This corresponded to an energy release of 30 kJ in PARKA. By bringing Godiva up to within 2.3 m of PARKA and with PARKA shut down and loaded to a reactivity of -$3.6, we later produced a yield of 1.4×10^{10} fissions per gram ^{235}U in pulses about 1 ms wide. The time profile of these pulses, measured with a fission chamber operating in the current mode, is shown in Fig. 20. It has thus been shown possible to produce peak power densities of 1500 W/g ^{235}U at the center of a test-pin bundle in PARKA. The width of these pulses can be increased by about a factor of 10 by setting PARKA control drums just subcritical. Peak power in the test region can be increased to 1.5×10^4 W/g in small test bundles by use of a polyethylene flux trap. It is felt that these peak power levels are in a range that may be useful for hodoscope transient testing and coded aperture evaluation.

Conclusion

Table 2 is a summary of results obtained so far by scanning with the hodoscope various-sized fuel bundles with a missing pin. The ability to detect one missing pin in an array of 127 is established, but there is an apparent trend towards obliteration of the image as the bundle size increases. It should be emphasized, moreover, that this static test of hodoscope resolution by no means establishes feasibility of detecting the loss of this quantity of material from a test assembly under dynamic conditions. It is rather a measure of the ultimate upper level for performance of hodoscopes on LMFBR fuel bundles of this size. Furthermore, the established limit should be applicable to any imaging system which depends upon self radiation as its source. It is not at all certain that it will be possible to detect a missing pin in a full 217- or 271-pin subassembly using the hodoscope technique or any other self-imaging technique under destructive test conditions.

TABLE 2
Relative Single-Pin Image Intensity as a Function of Test-Assembly Size

Number of Pins in Assembly	Single-Pin Fraction of Total Count Rate			
	$E_n > 1.3$ MeV	$E_n > 2.2$ MeV	$E_\gamma > 0.33$ MeV	$E_\gamma > 0.66$ MeV
1	0.33	0.43	0.45	0.54
37	0.054	0.070	0.046	0.059
91[a]	0.032		0.00	
127	0.018	0.020	0.010	0.010

[a] 91-Pin EBR-II Subassembly (Ref. 12)

References:

*Work supported by the U. S. Nuclear Regulatory Commission.

1. W. E. Stein, V. Starkovich, and J. D. Orndoff, "X-Ray Monitoring of Fuel Motion," in "Transactions of the Second Technical Exchange Meeting on Fuel-and Clad-Motion Diagnostics for LMFBR Safety Test Facilities," Report ANL/RAS 76-34 (1976)
2. G. T. Berzins, K. S. Han, and W. H. Roach, "Preliminary Report on the Pinex at TREAT," in "Transactions of the Second Technical Exchange Meeting on Fuel-and Clad-Motion Diagnostic for LMFBR Safety Test Facilities," Report ANL/RAS 76-34 (1976)
3. J. G. Kelly and K. T. Stalker, "ACPR Upgrade Fuel Motion Detection System" in "Transactions of the Second Technical Exchange Meeting on Fuel-and Clad-Motion Diagnostics for LMFBR Safety Test Facilities," Report ANL/RAS 76-34 (1976)
4. S. A. Wright and S. A. Dupree, "In-Core Fuel Motion Detection for Large Scale Tests," in "Transactions of the Second Technical Exchange Meeting on Fuel-and Clad-Motion Diagnostics for LMFBR Safety Test Facilities," Report ANL/RAS 76-34 (1976)
5. A. DeVolpi, R. J. Pecina, R. T. Daly, D. J. Travis, R. R. Stewart, and E. A. Rhodes, Nucl. Tech 27. 449 (1975)
6. H. U. Wider, M. G. Stevenson, and D. A. McArthur, "Material Diagnostic Requirements for STF," presentation at the NEA Specialist's Meeting on Fuel and Clad-Motion Diagnostics for Fast Reactor Safety Test Facilities. Los Alamos, New Mexico, 5-7 December 1977, (unpublished)
7. J. D. Orndoff and A. E. Evans, "STF Simulation with PARKA and Application to Diagnostic Instrumentation Evaluation, in "Transactions of the Second Technical Exchange Meeting on Fuel and Clad-Motion Diagnostics for LMFBR Safety Test Facilities," Argonne National Laboratory Report ANL/RAS 76-34 (1976)
8. T. R. Hill, "ONETRAN: A Discrete Ordinates Finite Element Code for the Solution of the One-Dimensional Multi-group Transport Equation," Los Alamos Scientific Laboratory report LA-5990-MS (June 1975)
9. W. F. Hornyak, Rev. Sci. Instr., 23, No. 6, 264 (1952)
10. H. O. Menlove, R. A. Forster, R. H. Augustson, A. E. Evans, and R. B. Walton, "Characteristics of ^{4}He Gas Tubes for Fast-Neutron Detection," Nuclear Safeguards Research and Development Program Status Report September-December, 1970, Los Alamos Scientific Laboratory report LA-4605-MS (1971) p 13
11. F. D. Brooks, Nucl. Instrum. Methods, 4, 151 (1959)
12. C. L. Fink, A. DeVolpi, E. A. Rhodes, and E. A. Evans, paper 2P-21, this symposium.